DNA Damage and Mutations Induced by Arachidonic Acid Peroxidation†

Punnajit Lim,‡ Kianoush Sadre-Bazzaz,‡ Jesse Shurter,‡ Alain Sarasin,§ and John Termini*,‡

Division of Molecular Biology, Beckman Research Institute of the City of Hope, 1450 East Duarte Road, Duarte, California 91010, and Institut Gustave Roussy, PR2, UPR 2169 CNRS, 39 rue Camille Desmoulins, 94805 Villejuif cedex, France

Received August 29, 2003; Revised Manuscript Received October 21, 2003

ABSTRACT: Endogenous cellular oxidation of ω6-polyunsaturated fatty acids (PUFAs) has long been recognized as a contributing factor in the development of various cancers. The accrual of DNA damage as a result of reaction with free radical and electrophilic aldehyde products of lipid peroxidation is believed to be involved; however, the genotoxic and mutation-inducing potential of specific membrane PUFAs remains poorly defined. In the present study we have examined the ability of peroxidizing arachidonic acid (AA, 20:4ω6) to induce DNA strand breaks, base modifications, and mutations. The time-dependent induction of single-strand breaks and oxidative base modifications by AA in genomic DNA was quantified using denaturing glyoxal gel electrophoresis. Mutation spectra were determined in XP-G fibroblasts and a repair-proficient line corrected for this defect by c-DNA complementation (XP-G$^+$). Mutation frequencies were elevated from ~5- to 30-fold over the background following reaction of DNA with AA for various times. The XPG gene product was found to be involved in the suppression of mutations after extended reaction of DNA with AA. Arachidonic acid-induced base substitutions were consistent with the presence of both oxidized and aldehyde base adducts in DNA. The frequency of multiple-base substitutions induced by AA was significantly reduced upon correction for the XPG defect (14% vs 2%, $P = 0.0015$). Evidence is also presented which suggests that the induced frequency of multiple mutations is lesion dependent. These results are compared to published data for mutations stimulated by α,β-unsaturated aldehydes identified as products of lipid peroxidation.

Epidemiological studies have suggested (*1*, *2*) and animal model and tissue culture studies have tended to support (*3*−*5*) a positive correlation between dietary intake of ω6-polyunsaturated fatty acids (PUFAs)[1] and increased risk for cancers of the colon, breast, and prostate. It is widely believed that enzymatic and nonenzymatic oxidation of dietary ω6 PUFAs within the phospholipid fraction of the nuclear envelope is genotoxic (*6*), and contributes to promotional events in carcinogenesis (*7*).

Arachidonic acid (AA, 20:4ω6) is one of the most important PUFAs in mammalian phospholipid membranes. It is distributed predominantly within membranes as an sn-2 phospholipid ester and is the sole biosynthetic precursor for the eicosanoid family of hormones. Various cellular stimuli mobilize phospholipase A2 (cPLA2) from the cytoplasm to the nuclear membrane, resulting in the hydrolytic release of AA. Oxidation of released AA by cyclooxygenase 2 (COX-2) or 5-lipoxygenase in the nuclear envelope is a key step in the biosynthesis of the 2-series prostaglandins and 4-series leukotrienes, respectively (*8*). Recent evidence has suggested that nuclear oxygenase activity may adventitiously result in the cooxidation of DNA via AA free radical intermediates (*9*). Moreover, a substantial fraction of deesterified AA evades the eicosanoid biosynthetic pathway and is oxidized by nonenzymatic free radical mechanisms (*10*). This may involve catalysis by low-valent transition-metal ions present in the nucleus such as iron and copper (*11*). These reactions also increase the potential for AA-induced DNA damage. Modest dietary supplementation with AA has been shown to dramatically increase membrane phospholipid AA levels in humans (*12*), which enhances cellular lipid peroxidation via these enzymatic and nonenzymatic pathways (*13*).

Potential DNA-damaging agents produced during lipid peroxidation include both free radical intermediates, primarily long-lived peroxyl radicals (*14*), and electrophilic aldehydes (*15*). Peroxyl radicals can initiate strand breaks and oxidative base modifications in DNA, and their mutagenic potential has been previously demonstrated in bacteria using model compounds (*16*, *17*). Aldehydes can condense with amine nucleophiles on DNA bases to form an array of cyclic and acyclic adducts (*18*−*20*). The mutation-inducing properties of several DNA aldehyde adducts have been described (*21*−*24*), but it is unclear to what extent these adducts contribute to the mutation profile induced by AA peroxidation.

To refine our understanding of the genotoxic and mutagenic potential of AA, we have examined the ability of peroxidizing AA to induce strand breaks and oxidative base

† Supported by NIH Grant GM59219 to J.T.

* To whom correspondence should be addressed. Phone: (626) 301-8169. Fax: (626) 301-8271. E-mail: jtermini@coh.org.

‡ Beckman Research Institute of the City of Hope.

§ Institut Gustave Roussy.

[1] Abbreviations: [1]PUFA, polyunsaturated fatty acid; AA, arachidonic acid; COX-2, cyclooxygenase 2; ABIP, 2,2′-azobis[2-(2-imidazolin-2-yl)propane] dihydrochloride; *supF*, suppressor F; XPG, xeroderma pigmentosum G gene; XP-G, xeroderma pigmentosum G complementation group; ssb, single-strand break; BER, base excision repair; NER, nucleotide excision repair; 4-HNE, 4-hydroxynonenal; MDA, malondialdehyde; Acr, acrolein; Cro, crotonaldehyde.

10.1021/bi035555w CCC: $25.00
Published on Web 11/27/2003

modifications in isolated genomic DNA, and to stimulate mutations in human cells using the pSP189 shuttle vector (*25*). Cells differing in the ability to carry out nucleotide excision repair due to XPG status were used to evaluate mutation spectra. This gene product is of particular interest since it has been shown to be involved in the repair of both bulky adducts (*26*, *27*) and oxidative DNA damage (*28*−*30*), and impaired function has been associated with the development of both external (*31*) and internal (*32*, *33*) cancers.

MATERIALS AND METHODS

Chemicals and Reagents. Arachidonic acid was obtained from Avanti Polar Lipids (Alabaster, AL). Purity was verified by ESI-MS in the negative ion mode. Radical initiators used to generate peroxyl radicals in the presence of O_2, 2,2′-azobis(2-amidinopropane) dihydrochloride (ABAP), and 2,2′-azobis[2-(2-imidazolin-2-yl)propane] dihydrochloride (ABIP) were obtained from Wako Chemicals (Richmond, VA).

Reaction of DNA with Peroxidizing AA and Peroxyl Radical Model Compounds. The reaction of pSP189 and human fibroblast DNA with ABAP or ABIP in the presence of O_2 was carried out as previously described (*34*). DNA reactions with arachidonic acid consisted of 10−20 μg of DNA, 3 μmol of AA (1 μL), and 1 nmol of Fe_2SO_4 (10 μL total volume). Emulsions were placed under an air atmosphere in an environmental shaker at 37 °C. Lipid peroxidation was allowed to continue for up to 16 h. Reactions were stopped by the addition of 90 μL of dd H_2O, followed immediately by extraction with 100 μL of $CHCl_3$ (2×) and hexane (1×). The organic layer was discarded, and the DNA was precipitated from the aqueous layer with 2.5 M ammonium acetate and 2.5 volumes of EtOH. The DNA pellet was washed with 70% EtOH and resuspended in 10 μL of H_2O to provide ∼5−10 μg/mL DNA.

Cell Lines. Fibroblasts derived from patients with the XP-G class 2 defect (XP3BR.SV) were used to examine mutations induced by lipid peroxidation. These cells express defective XPG proteins (*35*). Correction of this defect by c-DNA complementation (XP2BI-pXPG1) provided fibroblasts with a "normal" repair background. GM00637 human fibroblasts proficient in DNA repair were obtained from the Coriell Institute for Medical Research (Camden, NJ). All human fibroblast lines were SV40 immortalized. Cells were cultured in Dulbecco's modified Eagle's high glucose medium (Irvine Scientific, Santa Ana, CA) and supplemented with 4 mM L-glutamine, 100 units/mL penicillin G, 100 μg/mL streptomycin (Gibco Invitrogen Corp., Grand Island, NY), and 10% fetal bovine serum (Omega Scientific, Inc., Tarzana, CA). Cells were maintained in a 10% CO_2 atmosphere in a humidified incubator. To ensure plasmid maintenance, 0.5 mg/mL Geneticin (G-418 sulfate; Gibco Invitrogen) was added to the complemented XP2BI-pXPG1 cells.

Analysis of DNA Strand Breaks and Base Modifications Induced by Lipid Peroxidation. Human fibroblast DNA isolated from GM00637 cells was used to measure strand break densities induced by lipid peroxidation. Approximately 10^7 cells from freshly growing cultures or frozen cell pellets were suspended in 1 mL of buffer consisting of 10 mM Tris, 100 mM EDTA, pH 8.0, 100 μL of 10% SDS, and 50 μL of proteinase K (20 mg/mL). Lysed cells were incubated at 37 °C for 4−16 h and then extracted 2× with 1 mL of phenol-saturated chloroform. DNA was precipitated with 2.5 M ammonium acetate and 2.5 volumes of ethanol. The DNA pellet was washed with 80% ethanol and resuspended in 200 μL of TE. RNAse (2 μL, 1 mg/mL) was added and the resulting mixture incubated at 37 °C for 1 h. Genomic DNA was exposed to peroxidizing AA as described above. Strand breaks were induced at base-oxidized sites by treatment of 20 μg of peroxidized DNA with a mixture of Fpg (400 ng) and Nth (100 ng) proteins as previously described (*34*). Glyoxal denaturing gel electrophoresis was used to analyze the break patterns, and strand break densities were calculated from acridine orange stained gels using a Typhoon 9410 variable-mode imager (Amersham Biosciences) equipped with the ImageQuant software package (Molecular Dynamics, Sunnyvale, CA).

Shuttle Vector and Bacterial Strains Used for Mutation Detection. The shuttle vector pSP189 and *E. coli* indicator strain MBM7070 were kindly provided by Dr. Michael Seidman (*25*). The pSP189 plasmid contains the *supF* amber suppressor tRNA gene as the mutational marker, as well as sequences required for replication in both SV40 permissive cells and *E. coli*. The pSP189 vector also contains an 8-bp "signature sequence" at the 3′ end of the *supF* gene, which is a randomized element used to distinguish between clonal and independent mutants (*36*). The shuttle vector was isolated from *E. coli* MBM7070 and purified using CsCl/ethidium bromide gradient centrifugation. DNA was quantitated using UV absorbance spectrophotometry (1.0 OD = 50 μg/mL) and stored at 4 °C in ddd H_2O.

Fibroblast Transfection and Recovery of pSP189. Human fibroblasts were seeded ∼24 h prior to transfection (6×10^5 cells/100 mm plate). The nonliposomal FuGene 6 reagent (Roche Diagnostics, Indianapolis, IN) was used to transfect 5 μg of either the control or peroxidized plasmid DNA according to the instructions of the manufacturer. Cells were allowed to grow for 72 h at 37 °C prior to DNA isolation using the alkaline lysis method. Plasmid DNA was digested with 10 units of *Dpn*I at 37 °C for 30 min to eliminate unreplicated plasmids which retained the bacterial dam^+ methylation pattern. RNAse was then added and the incubation continued for another 30 min. Plasmid DNA was recovered by ethanol precipitation with glycogen, washed once with 70% ethanol, resuspended in 10 μL of H_2O, and quantitated by UV absorbance. Relative plasmid viability following reactions with AA was ascertained using an EGFP-expressing shuttle vector similar in size to pSP189 (pEGFP-Luc, Clontech). Fluorescence was quantified in XP-G cells by FACS analyses.

Bacterial Transformation and Mutant Selection. The mutations produced as a result of mammalian cell replication of peroxidized plasmids were recovered by "shuttling" the *supF*-containing pSP189 vector back into *E. coli* MBM7070. The MBM7070 strain carries *a lacZ*α gene interrupted by an amber codon. Plasmids with mutations in *supF* are unable to restore β-galactosidase activity, and thus appear as white or light blue colonies on X-gal chromogen-containing plates. MBM7070 was transformed via electroporation using a BioRad GenePulserII (Hercules, CA). Log-phase bacteria were rendered competent by a series of three cold washes in 10% (v/v) glycerol, and finally suspended in ice-cold 10%

glycerol at a concentration of (2−3) × 10^{10} cells/mL (1.0 $OD_{600} \approx 2.5 \times 10^8$ cells/mL). Approximately 0.1−0.5 μg (1 μL) of pSP189 DNA was electroporated using competent bacteria ((8−12) × 10^8 cells) in a 40 μL total volume in a 0.2 cm cuvette. The discharge voltage was 2.5 kV at a resistance of 200 Ω, and a capacitance of 25 μFD. Bacteria were incubated in SOC medium at 37 °C for 15 min prior to plating on LB agar supplemented with carbenicillin (120 μg/mL), X-gal (120 μg/mL; 5-bromo-4-chloro-3-indoyl β-D-galactopyranoside), and IPTG (40 μg/mL; isopropyl β-D-thiogalactopyranoside). The plates were incubated at 37 °C for 12−16 h prior to determination of the number of blue, light blue, or white colonies. The mutation frequency was calculated as the number of white and light blue colonies divided by the total number of colonies. Statistical significance was judged using the Fisher exact test.

Sequencing Analysis of supF Mutants. White and light blue colonies were purified by single-colony isolation and grown overnight in 5 mL of L-broth supplemented with 120 μg/mL carbenicillin. Cultures were incubated for an additional 4−5 h in the presence of chloramphenicol (170 μg/mL) to amplify the plasmid copy number. DNA was isolated using the QIAprep Spin Miniprep Kit (Qiagen, Valencia, CA). A primer (5′-GGCGACACGGAAATGTTGAA-3′), complementary to bases 4880−4900 of the pSP189 (+) strand was used for sequencing analysis (Genset, La Jolla, CA). All analyses were performed at the DNA Sequencing Core Facility of the City of Hope Cancer Center using an ABI 373 DNA sequencer (Applied Biosystems, Foster City, CA).

RESULTS

Quantitation of DNA Strand Breaks and Oxidized Bases Induced by Arachidonic Acid Peroxidation. Oxidizing radicals generated during lipid peroxidation may initiate DNA strand breaks by direct attack on the ribose phosphate backbone. Base oxidation can also occur, resulting in products which are potential substrates for base excision repair (BER) enzymes. Human fibroblast DNA was incubated for various times with AA stimulated to undergo peroxidation by the addition of catalytic Fe(II). The formation of frank strand breaks was monitored by denaturing glyoxal agarose gel electrophoresis. The integrated fluorescence intensities of acridine orange stained gels were used to calculate single-strand break densities. To estimate the extent of base modification, aliquots of DNA were withdrawn at different time points and digested with a mixture of Fpg and Nth proteins under enzyme-saturating conditions as previously described (*34*). Since these proteins possess both DNA glycosylase and AP lyase activities, additional strand breaks were created at base-oxidized sites. Quantitation of break densities induced by BER enzyme treatment followed by correction for frank strand breaks yields minimum estimates of the extent of base oxidation.

A typical gel result is shown in Figure 1A. Lanes 3−6 reveal that incubation of genomic DNA with Fe(II) alone in the absence of lipid did not induce strand breaks. DNA damage was only observed upon the addition of AA, as shown in lanes 7−10. Thus, free radicals associated with lipid peroxidation, rather than adventitious Fenton chemistry, were solely responsible for the measured strand breaks. The autoxidation of arachidonic acid also gave rise to DNA strand

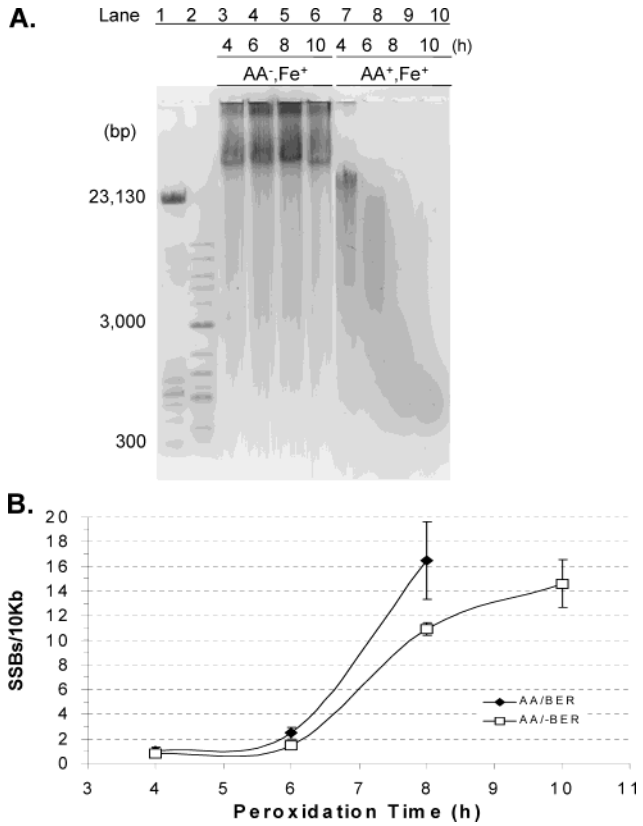

FIGURE 1: Quantitation of ssb's and base modifications induced by AA in genomic DNA. (A) Denaturing glyoxal gel analysis of AA-induced single-strand breaks: lanes 1 and 2, λ-*Hin*dIII+ΦX174-*Hae*III digest, 1 kb + 100 bp ladder; lanes 3−6, incubation of 10 μg of genomic DNA with 100 μM Fe_2SO_4 in the absence of AA for 4−10 h; lanes 7−10, same as lanes 3−6 with the addition of 3 μmol of AA. (B) Calculated strand break densities derived from glyoxal gel analyses. Data represent the average of three determinations. Squares denote the frank strand breaks produced by AA peroxidation at the indicated times (h). Filled diamonds represent the sum of frank strand breaks and breaks induced by reaction with Fpg and Nth base excision repair (BER) proteins.

breaks, although with substantially slower reaction kinetics due to the absence of Fe(II) catalyst (data not shown). The molecular weight markers in lanes 1 and 2 were used to calibrate band migration distances, and the molecular weight distribution of fragments within each lane was used to compute the strand break densities as previously described (*34*). Plots of strand break densities representing frank and BER-induced breaks are presented in Figure 1B. The lower curve represents the frank strand breaks generated by AA peroxidation. The upper curve represents the total break densities resulting from frank strand breaks and BER-induced cleavages at modified bases and abasic sites.

Detectable frank strand breaks initially appeared after 4 h of reaction, followed by a lag phase lasting up to ~6 h. This was followed by a sharp increase in strand breaks and base modifications from 6 to 8 h. The rate of increase of base modifications appears greater than for single-strand breaks (ssb's) over this period. At 8 h the mean value of frank strand breaks from three independent determinations was ~1.1 ssb's/kb, while the total number of BER-induced + frank breaks was found to be ~1.6 ssb's/kb. The difference between values in the upper and lower curves at a particular time point provides a minimum estimate of the extent of oxidative base modifications resulting from AA peroxidation.

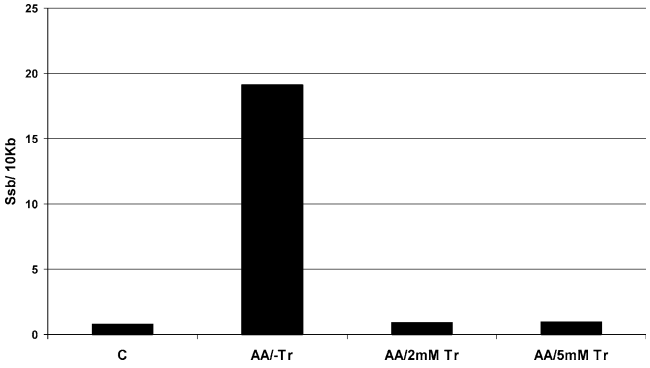

FIGURE 2: Inhibition of AA-induced ssb's by Trolox. Genomic DNA was incubated with Fe_2SO_4 in the presence (AA/−Tr) or absence (C) of AA for 8 h. Addition of 2 or 5 mM Trolox inhibited breaks to levels comparable to those of the controls.

This estimate is considered to be minimal since it is assumed that not all peroxidation-induced base damage is recognizable by Fpg and Nth proteins. These values provide a lower estimate of ~5 base modifications/10^4 nt upon reaction of DNA with peroxidizing AA for 8 h. It was not possible to accurately measure BER-induced strand breaks beyond this time point, since fragment distributions which would give rise to break densities >2 kb^{-1} could not be quantitatively resolved.

Direct evidence for a role of oxidative radicals in AA-induced DNA damage was obtained using Trolox, a water-soluble vitamin E analogue commonly used as a trap for peroxyl radicals (*37*). Strand break densities were measured following reactions of genomic DNA with AA for 10 h in the presence of 2 or 5 mM Trolox. These results are shown in Figure 2. In the absence of Trolox, strand break densities induced by AA peroxidation were similar to those measured in Figure 1B. The addition of 2 or 5 mM Trolox to the Fe(II)-catalyzed reaction inhibited peroxidation-induced strand breaks to a level comparable to control incubations in the absence of lipid.

Arachidonic Acid-Induced Mutations in XP-G/XP-G$^+$ Cells. The ability of DNA damage induced by AA peroxidation to induce mutations following replication in human cells was examined using the pSP189 shuttle vector bearing the *supF* tRNA mutational marker. Plasmids exposed to AA peroxidation for 4, 8, and 16 h were transfected into an XPG-deficient cell line (XP-G, class 2), and the mutation frequencies were determined. Relative plasmid viability following reaction with AA for 4, 8, and 16 h was ~ 30%, 20%, and 5%, respectively. Arachidonic acid-induced mutations were also measured in XP-G class 2 cells corrected for this NER defect by c-DNA complementation (XP-G$^+$). Following replication of pSP189 in XP-G or XP-G$^+$ cells for 72 h, plasmids were isolated and transformed into an amber suppressor *E. coli* strain MBM7070. Mutation frequencies measured for XP-G and XP-G$^+$ lines are plotted in Figure 3.

Mutation frequencies in Figure 3 represent the results of three or more independent experiments. Background mutation frequencies were determined in each cell line by transfection with unreacted pSP189. More than 20000 colonies were screened for each XP-G and complemented XP-G$^+$ line to establish the background mutation frequencies. These were the same within experimental error, suggesting that the XP-G defect did not elevate the mutation background in the absence of DNA damage. Plasmids incubated with Fe_2SO_4 in the absence of AA for the same time periods did not increase the background mutation frequencies following transfection and replication in fibroblasts (data not shown). This indicated that Fe(II) alone did not promote any detectable mutagenic DNA damage, consistent with the data in Figure 1.

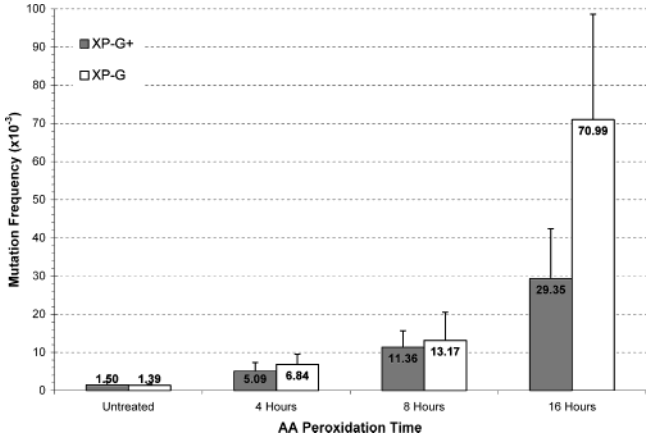

FIGURE 3: SupF mutation frequencies in XP-G and XP-G$^+$ fibroblasts induced by transfection of the pSP189 shuttle vector following reaction with peroxidizing AA for the indicated times. Background mutation frequencies were determined by transfection of untreated pSP189.

On average, 25000 colonies were screened for each time point to calculate lipid peroxidation-induced mutation frequencies. The mutation frequencies in both XP-G and XP-G$^+$ cell lines increased with the extent of lipid peroxidation. Exposure of pSP189 to AA peroxidation for 4 h prior to transfection increased the mutation frequency 5-fold relative to the background in the XP-G fibroblasts. Increasing the AA peroxidation time to 8 h resulted in ~8- and 10-fold increases in mutation frequencies relative to the uninduced background for XP-G$^+$ and XP-G cells, respectively. No significant differences in mutation frequencies were detected between cell lines following reaction with AA for 4 or 8 h. However, after reaction for 16 h a more than 2-fold difference in mutation frequencies between XP-G and XP-G$^+$ lines was observed ($p = 0.001$). The mutation frequency in XP-G cells obtained after 16 h of reaction with AA was elevated 50-fold over the background. This was the only reaction condition that produced a statistically significant difference in mutation frequencies between XP-G and XP-G$^+$ cells.

Classes of Mutations Produced in XP-G and XP-G$^+$ Fibroblasts by Peroxidizing AA and Peroxyl Radical Model Compounds. The different classes of mutations observed upon the induction of DNA damage by AA in XP-G/XP-G$^+$ cells are provided in Table 1. Data in Tables 1 and 2 for AA in either repair-defective or complemented cells was compiled from 4, 8, and 16 h reactions, since the distribution of mutations within each cell line did not vary significantly with peroxidation time (data available as Supporting Information). The XP-G/XP-G$^+$ spontaneous mutation profiles as well as mutations induced by the peroxyl radical model system ABIP/O_2 in XP-G cells are also provided in Table 1.

In the NER-defective line, single-base substitutions accounted for 67% of all AA mutations, significantly lower than the 88% observed in the repair-competent fibroblasts

Table 1: Classification of Mutations in pSP189 Replicated in Human Cells

	XP-G[a] cell line			XP-G$^+$ cell line	
	no mutagen	AA	ABIP/O_2[c]	no mutagen	AA
independent plasmids analyzed	33 (100)	109 (100)	66 (100)	30(100)	49 (100)
point mutations					
single-base substitutions	26 (79)	73 (67)[d]	57 (86)	24 (80)	43 (88)
tandem-base substitutions	0	1 (1)	2 (3)	0	1 (2)
multiple-base substitutions	3 (9)	15 (14)[e]	3 (4.5)[f]	3 (10)	1 (2)
deletions	4 (12)	18 (16)	3 (4.5)[g]	3 (10)	4 (8)
insertions	0	0	0	0	0
deletions/insertions	0	1 (1)	0	0	0
others[b]	0	1 (1)	1 (2)	0	0

[a] Number of independent plasmids with alterations (%). [b] AA, rearranged sequence; ABIP/O_2, multiple alterations involving deletion, insertion, and base substitution in a single clone. [c] The mutation frequency induced by reaction with 1 mM ABIP in an O_2-saturated solution for 1 h was 48×10^{-3}. [d] $P = 0.0003$ versus XP-G$^+$ cells. [e] $P = 0.0015$ versus XP-G$^+$ cells. [f] $P = 0.026$ versus AA in XP-G cells. [g] $P = 0.009$ versus AA in XP-G cells.

Table 2: Distribution of Base Substitution Mutations in pSP189 Replicated in Human Cells

	XP-G[a] cell line			XP-G$^+$ cell line	
	no mutagen	AA	ABIP/O_2	no mutagen	AA
transitions	7 (22)	47 (44)	6 (9)	12 (40)	21 (45)
G:C → A:T	7 (22)	43 (41)	6 (9)	11 (37)	20 (43)
A:T → G:C	0	4 (4)	0	1 (3)	1 (2)
transversions	25 (78)	59 (56)	62 (91)	18 (60)	26 (55)
G:C → T:A	18 (56)	43 (41)	31 (46)	11 (37)	22 (47)
G:C → C:G	7 (22)	11 (10)	29 (43)	7 (23)	3 (6)
A:T → T:A	0	4 (4)	1 (1)	0	1 (2)
A:T → C:G	0	1 (1)	1 (1)	0	0
total	32 (100)	106 (100)	68 (100)	30 (100)	47 (100)

[a] Number of mutations (%).

($P = 0.0003$). This difference was mainly due to the increased frequency of multiple mutations in the XP-G fibroblasts. A striking percentage (14%) of AA-induced base substitutions in the XP-G cells were detected as multiples, i.e., nontandem mutations produced within a single-mutant clone. Complementation of the XPG defect significantly reduces the frequency of multiples induced by AA (2%, $P = 0.0015$), suggesting a role for diminished XPG activity in the generation of multiples. Compared to the level of stimulation by AA, the frequency of multiples was significantly diminished in XP-G cells when ABIP/O_2 was used to induce DNA damage (4.5%, $P = 0.026$). Tandem mutations, potentially induced by vicinal DNA damage, occurred at $\leq$2% frequency in the AA-induced mutants in both cell lines. The differences in AA-induced deletion frequencies between XP-G and XP-G$^+$ lines were not found to be statistically significant. However, ABIP/O_2-induced DNA damage resulted in a significantly smaller percentage of deletions relative to that for AA in XP-G cells (4.5% vs 16%, $P = 0.009$). These results within XP-G cells suggest that the frequency of multiple mutations and deletions is dependent upon the nature of the DNA damage. The distributions of spontaneous mutation classes in the XP-G and XP-G$^+$ cells were virtually identical, in contrast to the mutagen-induced pattern.

Distribution of Base Substitution Mutations in XP-G and XP-G$^+$ Cells. The distributions of all base substitution mutations are provided in Table 2. The percentage of transversions (56%) and transitions (44%) induced by AA in the XP-G fibroblasts was essentially the same as that observed in the complemented line. The distribution of individual classes of AA-induced transitions and transversions was also remarkably similar for both cell lines. For example, GC to AT transitions occurred at a frequency of 41% and 43% in XP-G and XP-G$^+$ cells, respectively, while the AT to GC transition frequencies were 4% and 2%. Among AA-induced transversions, GC to TA predominated to the extent of 41% and 47% in XP-G and XP-G$^+$ lines, respectively. The percentages of GC to CG transversions were also similar.

These patterns were distinctly different from those of the peroxyl-radical-model-compound-induced mutation spectra determined in XP-G cells. DNA damage by ABIP/O_2-induced G transversions almost exclusively (91%). GC to TA and GC to CG mutations were observed in equal proportions. This 1:1 distribution of G transversions was also observed in the ABAP/O_2-induced mutation spectra previously reported in *E. coli* using the *lacZ*α reporter system (*17*). This same pattern was also observed in XP-A, XP-F, and GM00637 human fibroblasts using either the ABAP or ABIP initiator in the presence of O_2 (data not shown).

Mapping of Base Substitution Mutations within the supF Locus Induced by AA and Peroxyl Radical Model Compounds in XP-G Cells. A sequence map of AA-induced base substitution mutations acquired in XP-G cells is presented in Figure 4A. The *supF* tRNA gene sequence is shown in bold. The AA-induced base substitutions are denoted above while those arising spontaneously following transfection of unreacted pSP189 are indicated below the *supF* sequence. The ABIP/O_2-induced base substitution map acquired in XP-G cells is also presented in Figure 4B. A number of mutation "hot spots" can be observed in the AA-induced spectra of Figure 4A. These are defined as five or more mutations at a specific base position, and represent a significant deviation from a random distribution. Examples of these in the AA-induced spectra include $(GC)_{57,92}$ and $(CG)_{61,67,77,83,91}$.

Multiple and tandem base substitutions detected within the same clone are grouped by color in Figure 4. With one exception, all of the multiples were observed as double-base substitutions. The exception was an unusual quadruple-base substitution mutant observed in the AA-induced mutation spectra consisting of $(CG)_{74}$ to AT, $(CG)_{77,83}$ to TA, and $(CG)_{91}$ to GA substitutions (Figure 4A). The spacing between multiple-base substitutions was between 2 and 34 nt in nearly all examples (14 out of 15). The double mutation $(CG)_{61,77}$ to (AT) was unique in that it was observed in four independent clones (4 out of 15, 27%). The sequence map of ABIP/O_2-induced base substitutions in XP-G cells is presented in Figure 4B. Fewer hot spots were observed in the ABIP/O_2-induced pattern; however, a strong hot spot was observed at $(CG)_{100}$.

The location and sizes of the spontaneous and induced pSP189 deletions are provided in the Supporting Information. The sizes of the deletion fragments in the majority (12 out

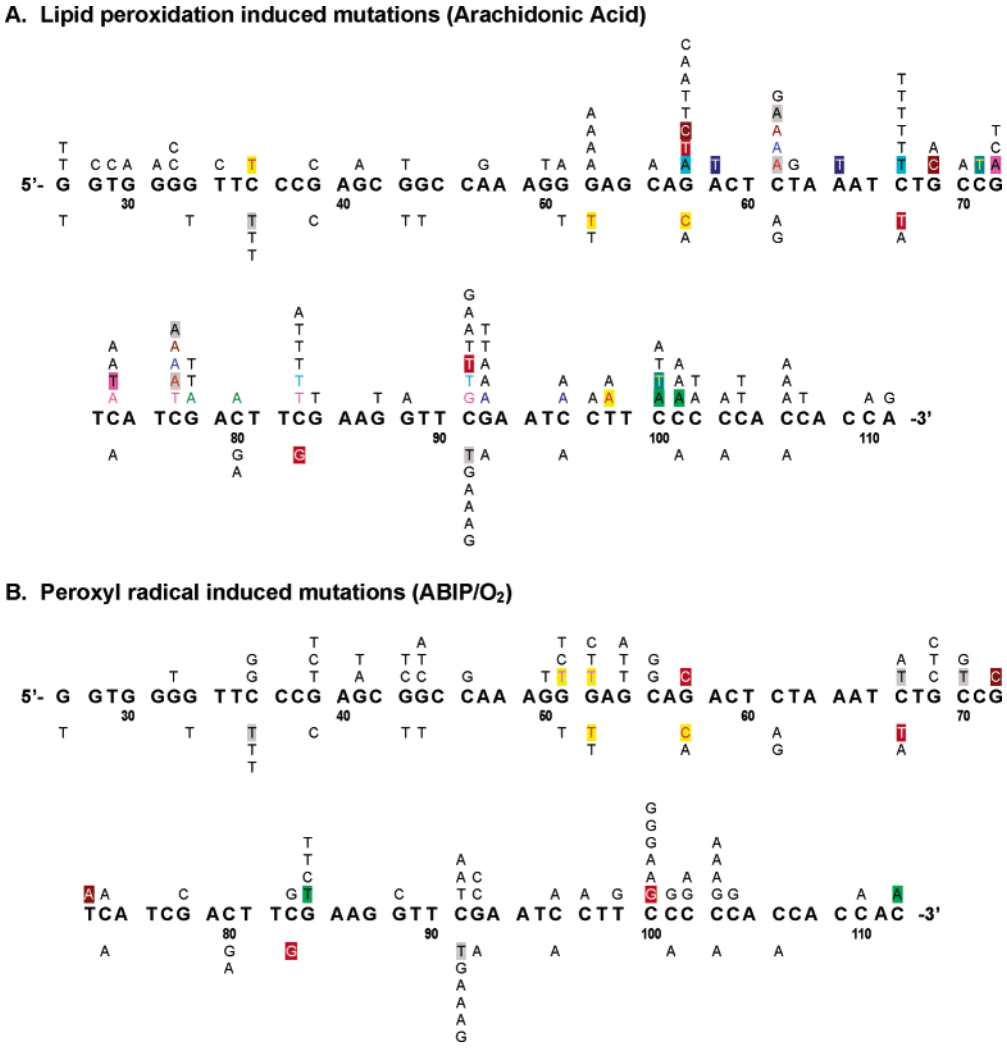

FIGURE 4: Sequence distribution of supF base substitution mutations obtained in XP-G cells. The numbering follows the Genbank annotation for pSP189 plasmid (U14594.1). The supF sequence is shown in bold. Letters above the sequence indicate substitutions induced by AA (A) or ABIP/O_2 (B). The spontaneous background substitutions in supF following transfection of unreacted plasmids are denoted below the sequence. Multiple and tandem base substitutions occurring within the same clone are grouped by color.

of 18) of examples induced by AA in XP-G were >100 nt. Deletions occurred between direct repeats of 2−5 bases in 11 out of 18 cases. No AA-induced single-base deletions were detected in either cell line; however, these were observed in the ABIP/O_2-induced mutation spectra (two out of three).

DISCUSSION

Although the genotoxicities of reactive intermediates associated with lipid peroxidation such as peroxyl radicals and lipid-derived aldehydes have been studied in detail, information concerning the mutation-inducing potential of specific PUFAs in human cells has not been available. Reaction of the pSP189 shuttle vector with AA for 4 or 8 h led to comparable increases in the observed mutation frequencies for XP-G and XP-G$^+$ cells. However, extending the peroxidation time to 16 h led to a significant difference in the mutation frequencies between these lines (Figure 3). These observations would be consistent with the accumulation of XPG addressable lesions following prolonged reaction with AA. Alternatively, the residual repair activity of the defective XPG gene product for AA-induced DNA damage may become saturated at high doses.

The XPG gene product is an endonuclease which initiates repair patch excision ~5 nt to the 3′ side of DNA lesions during NER (*38*). In addition to its well-known function in the repair of bulky adducts, a role for XPG in the repair of oxidative DNA damage has also been described (*28*−*30*). Cells used in this study belong to the XP-G class 2 type. XPG proteins are produced in these cells; however, the product from one allele is severely truncated, while the other product contains mutations which severely impair the endonuclease activity (*35*). The ability to repair oxidized purines is compromised, but not completely absent, in XP-G class 2 cells (*30*). Thus, XPG may be involved in the suppression of mutations caused by both aldehyde adducts and oxidative damage induced by AA peroxidation.

The data in Figure 1 demonstrate that peroxidizing AA can efficiently induce single-strand breaks in genomic DNA. The lag period observed preceding the rapid increase in strand breaks and base oxidation likely reflects the induction period for propagation of peroxidation. Qualitatively similar lag phases have been observed in the kinetics of linolenic acid (18:3ω6) peroxidation (*39*). Evidence that strand breaks were induced by free radicals was provided by Trolox inhibition (Figure 2). Intermediates responsible for the

induced strand breaks are most likely AA peroxyl radicals (AAOO•). Induction of single-strand breaks in genomic DNA using the ABAP/O_2 peroxyl radical-generating reaction has previously been described (*34*). It is formally possible that AA-derived alkoxyl radicals (AAO•) may also be involved in free-radical-induced DNA damage; however, due to the rapid rate of intramolecular cyclization by PUFA alkoxyl radicals, their free concentration is believed to be low during lipid peroxidation (*40*).

Oxidative base modifications in genomic DNA induced by AA peroxidation were quantified using a combination of Fpg and Nth glycosylases, enzymes which recognize oxidized purines and pyrimidines, respectively. The identities of the oxidized bases are currently under investigation; however, it is likely that 8-oxoguanine (8-oxoG) and secondary oxidation products such as oxazolone are produced. Reaction of calf thymus DNA with AA-containing liposomes has been previously shown to stimulate formation of 8-oxoG (*41*). Reaction of dGpdT with ABAP/O_2 peroxyl radical model compounds has been shown to give rise to 8-oxoG- and oxazolone-containing products (*42*). The presence of these lesions in the pSP189 shuttle vector could explain some features of the AA-induced mutation spectrum. 8-oxoG (*43*) and its secondary oxidation products (*44*, *45*) give rise primarily to GC to TA and GC to CG transversions. However, oxidized guanines cannot account for GC to AT transitions, observed at a frequency of ~40% in the AA-induced mutation spectra (Table 2). The cytosine-derived oxidation products 5-hydroxycytosine (5-OH-C), 5-hydroxyuracil, and uracil glycol, are candidate lesions for the generation of this mutation (*46*, *47*). However, GC to AT transitions comprise only a minor fraction (9%) of the ABIP/O_2-induced spectra, which suggests that base oxidation makes at best only a modest contribution to this substitution mutation.

This transition is also induced by etheno adducts of guanine (*21*) and cytosine (*48*). Etheno adducts may be formed via reaction of DNA with 2,3-epoxy-4-hydroxynonanal, a 4-hydroxynonenal (4-HNE) oxidation product generated during lipid peroxidation (*18*, *49*) or via condensation with activated electrophiles produced from oxidative degradation of deoxyribose (*49*, *50*). Cyclic propano adducts formed from the reaction of DNA with malondialdehyde (MDA) are not expected to play a role in AA-induced genotoxicity, since MDA is only formed in trace amounts during AA peroxidation (*51*). Thus, the AA-induced mutation pattern is consistent with the presence of both oxidized and aldehyde adducted bases in the pSP189 shuttle vector. Attempts to quantify etheno adducts in DNA, using either the AlkA or hMPG proteins (*52*, *53*), yielded inconsistent results (data not shown).

GC/MS analyses of aldehydes produced during AA peroxidation has identified 4-HNE and acrolein (Acr) as potential DNA electrophiles (*51*−*54*). Mutation spectra induced upon reaction of 4-HNE (*55*) and Acr (*56*) with the pSP189 shuttle vector have recently been reported, so these results may be directly compared with our data. In both the Acr- and 4-HNE-induced mutation spectra, GC to TA transversions predominated at a frequency approximately twice that of GC to AT transitions. In the AA-induced spectra these mutations occurred at approximately equal frequencies. An unusually high percentage of tandem mutations was

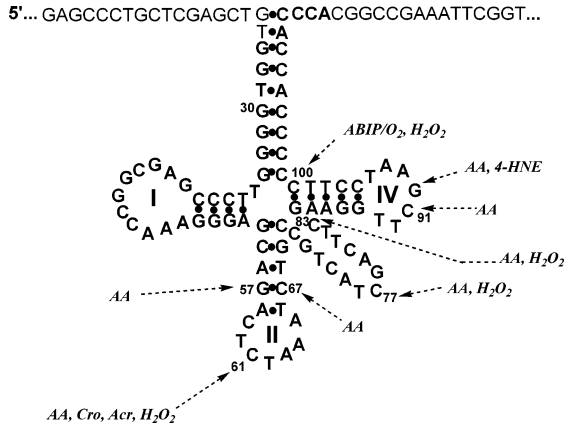

FIGURE 5: Hot spots observed for the supF tRNA gene (boldface) in pSP189 mapped onto a hypothetical secondary structure. Arrows correspond to hypermutagenic sites detected for AA and ABIP/O_2 (this work), as well as H_2O_2 (*59*), Acr (*56*), HNE (*55*), and Cro (*58*).

observed upon treatment of pSP189 with Acr (12%) or 4-HNE (19%), whereas this class of mutations was observed only rarely in the AA-induced mutation spectra (≤2%) in XP-G and XP-G^+ fibroblasts. Tandem mutations have been proposed to be a common feature of α,β-unsaturated-aldehyde-induced mutagenesis due to the formation of cross-linked lesions between neighboring bases (*56*). Interestingly, the only *supF* tandem mutation detected in the AA-induced mutation spectra at $(CG)_{100,101}$ (Figure 4a) was also observed in the 4-HNE spectra acquired in XP-A cells. Although 4-HNE can react with base nucleophiles to form saturated cyclopropano adducts and cross-links (*57*), the abundance of GC to AT transitions and the lack of significant levels of tandems in the AA-induced spectra suggest that the reaction of 2,3-epoxy-4-hydroxynonanal may efficiently compete with 4-HNE condensation, yielding predominantly etheno adducts.

Some of the hot spots observed in the AA- and ABIP/O_2-induced mutation spectra in Figure 4 have been previously reported in the literature for other mutagens. For example, the AA hot spot at $(CG)_{61}$ has also been identified in crotonaldehyde (Cro)-induced (*58*), Acr-induced (*56*), and H_2O_2-induced (*59*) *supF* mutation spectra. The $(CG)_{77,83}$ hot spots were observed in both AA- and H_2O_2-induced mutation spectra, whereas the $(CG)_{100}$ hot spot was a common feature of ABIP/O_2 and H_2O_2 treatment. A 4-HNE hot spot at $(GC)_{92}$ also appears in the AA-induced spectra. We suggest that these common hot spots reflect sites along the *supF* gene which are hyperreactive toward attack by free radicals and electrophilic agents. Although it is unclear to what extent the *supF* gene deviates from a canonical B-helix, mapping hot spots onto a hypothetical secondary structure resembling tRNA reveals some common features of the hyperreactive sites (Figure 5). In this representation, hypermutagenic sites correspond to positions predicted to be either single stranded or at boundary regions between discrete secondary structural features. Thus, hot spots at 61, 77, 91, and 92 occur within loop regions, whereas those at 57, 67, 83, and 100 occur at or adjacent to helix−loop or helix−helix boundary regions. Unusual DNA secondary structure has been previously proposed to explain the H_2O_2-induced hot spot at $(CG)_{100}$ in *supF* (*60*).

Arachidonic acid peroxidation induced multiple mutations within the *supF* gene at relatively high frequencies (14%).

Correction of the XPG defect by c-DNA complementation significantly reduced the frequency of multiples (2%, $P = 0.0015$). Multiple mutations may have resulted from the failure to remove multiple lesions due to the loss of XPG endonuclease activity. Lipid-peroxidation-induced multiple lesions could occur in DNA even at low concentrations of PUFAs. This is because PUFA decomposition results in the generation of multiple reactive intermediates such as peroxyl radicals and aldehydes at potentially high local concentrations. This is in contrast to single-hit reactive intermediates, e.g., •OH, which would be predicted to induce multiple lesions in a strictly concentration-dependent manner.

Seidman has proposed that multiple mutations may result from successive misincorporations by error-prone polymerases during excision patch repair, rather than from multiple lesions (*61*). In support of this hypothesis, a single-strand nick introduced enzymatically in *supF* as a model lesion induced a 3-fold increase in the frequency of multiple mutations in XP-A cells (*61*). Since AA can induce ssb's, it would appear possible that this mechanism could account for some percentage of multiples observed in our study. The lack of a one to one correspondence between lesions and observed mutations demanded by this mechanism implies that single-base substitution and multiple mutations should occur at different sites. This was observed in the UV-induced mutation spectra (*61*). However, it can be seen from the data in Figure 4A that the AA-induced multiples in XP-G cells coincide extensively with the single-base substitutions.

DNA damage induced by the ABIP/O_2 system did not stimulate the production of multiple mutations in XP-G cells. Since these peroxyl radical model compounds efficiently induce ssb's in a dose-dependent manner (*34*), this would suggest that ssb's are not sufficient for the induction of multiple mutations in XP-G cells. The failure to stimulate multiples may be a general feature of oxidative DNA damage. Multiples in *supF* were not detected in the Cu(II)/H_2O_2-induced mutation spectra determined in XP-A cells (*62*). However, multiples appear to be a common feature of UV-induced mutation spectra in *supF* in a variety of different cell lines, including XP-A (*61*, *63*, *64*). Thus, the induction of multiple mutations is likely lesion dependent. Bulky lesions such as UV photoproducts and possibly aldehyde DNA adducts (*56*, *58*) appear to stimulate the formation of multiple mutations. It has been hypothesized that the accumulation of multiple mutations plays a role in hypermutagenesis of p53, and thus, this phenomenon may be of particular importance in the development of various cancers (*65*, *66*). Their relatively common occurrence in *supF* in response to certain mutagens suggests multiples may play a more general role in hypermutation phenomena.

The induced deletion frequencies demonstrated mutagen dependence, but did not appear to be linked to XPG status. It is possible that the size of the deleted fragments may depend on the XPG status; however, additional deletion mutants in XP-G^+ cells need to be characterized to make this determination. Single-base deletions were only observed in the ABIP/O_2-induced spectra. These have been shown to be a prominent feature of H_2O_2-induced mutation spectra (60% of all deletions), suggesting an association with oxidative DNA damage (*67*).

Our results demonstrate that AA peroxidation can efficiently induce mutations in mammalian cells and promote DNA strand breaks. These results tend to support the hypothesis that increased cellular levels of AA may exert genotoxic effects and elevate cancer risk. In particular, the stimulation of multiple-base substitutions and large deletions observed in XP-G cells suggests that individuals with inherited or somatic NER defects may be particularly sensitive to the genotoxic and mutagenic effects of arachidonic acid peroxidation.

ACKNOWLEDGMENT

We thank Dr. P. K. C. Cooper (University of California, Berkeley) for the gift of XP-G/XP-G^+ human cell lines. The experimental assistance of Vanessa Holland and helpful discussions with Dr. Adam Bailis are gratefully acknowledged.

SUPPORTING INFORMATION AVAILABLE

Time-dependent distribution of AA-induced mutations in XP-G/XP-G^+ cells, as well as the sizes and location of AA- and ABIP/O_2-induced deletion fragments obtained in XP-G and XP-G^+ cells. This material is available free of charge via the Internet at http://pubs.acs.org.

REFERENCES

1. Pearce, M. L., and Dayton, S. (1971) *Lancet 1*, 464−467.
2. Rose, D. P., Boyar, A. P., and Wynder, E. L. (1986) *Cancer 58*, 2363−2371.
3. Welsch, C. W. (1995) *Free Radical Biol. Med. 18*, 757−773.
4. Rose, D. P. (1997) *Am. J. Clin. Nutr. 66*, 1513S−1522S.
5. Klurfeld, D. M., and Bull, A. W. (1997) *Am. J. Clin. Nutr. 66*, 1530S−1538S.
6. Marnett, L. J., and Plastaras, J. P. (2001) *Trends Genet. 17*, 214−221.
7. Bartsch, H., Nair, J., and Owen, R. W. (1999) *Carcinogenesis 20*, 2209−2218.
8. Funk, C. D. (2001) *Science 294*, 1871−1875.
9. Nikolic, D., and van Breemen, R. B. (2001) *Chem. Res. Toxicol. 14*, 351−354.
10. Morrow, J. D., Hill, K. E., Burk, R. F., Nammour, T. M., Badr, K. F., and Roberts, L. J., 2nd. (1990) *Proc. Natl. Acad. Sci. U.S.A. 87*, 9383−9387.
11. Stohs, S. J., and Bagchi, D. (1995) *Free Radical Biol. Med. 18*, 321−336.
12. Nelson, G. J., Schmidt, P. C., Bartolini, G., Kelley, D. S., Phinney, S. D., Kyle, D., Silbermann, S., and Schaefer, E. J. (1997) *Lipids 32*, 427−433.
13. Ferretti, A., Nelson, G. J., Schmidt, P. C., Kelley, D. S., Bartolini, G., and Flanagan, V. P. (1997) *Lipids 32*, 435−439.
14. Marnett, L. J. (1987) *Carcinogenesis 8*, 1365−1373.
15. Esterbauer, H., Schaur, R. J., and Zollner, H. (1991) *Free Radical Biol. Med. 11*, 81−128.
16. Harkin, L. A., Butler, L. M., and Burcham, P. C. (1997) *Chem. Res. Toxicol. 10*, 575−581.
17. Valentine, M. R., Rodriguez, H., and Termini, J. (1998) *Biochemistry 37*, 7030−7038.
18. el Ghissassi, F., Barbin, A., Nair, J., and Bartsch, H. (1995) *Chem. Res. Toxicol. 8*, 278−283.
19. Kasai, H., Iwamoto-Tanaka, N., and Fukada, S. (1998) *Carcinogenesis 19*, 1459−1465.
20. Marnett, L. J. (1999) *Mutat. Res. 424*, 83−95.
21. Cheng, K. C., Preston, B. D., Cahill, D. S., Dosanjh, M. K., Singer, B., and Loeb, L. A. (1991) *Proc. Natl. Acad. Sci. U.S.A. 88*, 9974−9978.
22. Shibutani, S., Suzuki, N., Matsumoto, Y., and Grollman, A. P. (1996) *Biochemistry 35*, 14992−14998.
23. Fink, S. P., Reddy, G. R., and Marnett, L. J. (1997) *Proc. Natl. Acad. Sci. U.S.A. 94*, 8652−8657.
24. Levine, R. L., Yang, I. Y., Hossain, M., Pandya, G. A., Grollman, A. P., and Moriya, M. (2000) *Cancer Res. 60*, 4098−4104.
25. Kraemer, K. H., and Seidman, M. M. (1989) *Mutat. Res. 220*, 61−72.

26. Huang, J. C., Svoboda, D. L., Reardon, J. T., and Sancar, A. (1992) *Proc. Natl. Acad. Sci. U.S.A. 89*, 3664−3668.
27. Moggs, J. G., Yarema, K. J., Essigmann, J. M., and Wood, R. D. (1996) *J. Biol. Chem. 271*, 7177−7186.
28. Cooper, P. K., Nouspikel, T., Clarkson, S. G., and Leadon, S. A. (1997) *Science 275*, 990−993.
29. Klungland, A., Hoss, M., Gunz, D., Constantinou, A., Clarkson, S. G., Doetsch, P. W., Bolton, P. H., Wood, R. D., and Lindahl, T. (1999) *Mol. Cell 3*, 33−42.
30. Le Page, F., Kwoh, E. E., Avrutskaya, A., Gentil, A., Leadon, S. A., Sarasin, A., and Cooper, P. K. (2000) *Cell 101*, 159−171.
31. Emmert, S., Schneider, T. D., Khan, S. G., and Kraemer, K. H. (2001) *Nucleic Acids Res. 29*, 1443−1452.
32. Kraemer, K. H., Lee, M. M., and Scotto, J. (1984) *Carcinogenesis 5*, 511−514.
33. Cheng, L., Spitz, M. R., Hong, W. K., and Wei, Q. (2000) *Carcinogenesis 21*, 1527−1530.
34. Rodriguez, H., Valentine, M. R., Holmquist, G. P., Akman, S. A., and Termini, J. (1999) *Biochemistry 38*, 16578−16588.
35. Lalle, P., Nouspikel, T., Constantinou, A., Thorel, F., and Clarkson, S. G. (2002) *J. Invest. Dermatol. 118*, 344−351.
36. Parris, C. N., and Seidman, M. M. (1992) *Gene 117*, 1−5.
37. Shane, R. A., and Ingold, K. U. (2002) *Chem. Res. Toxicol. 15*, 1324−1329.
38. Mu, D., Hsu, D. S., and Sancar, A. (1996) *J. Biol. Chem. 271*, 8285−8294.
39. Cho, S.-Y., Miyashita, K., Miyazwa, T., Fujimoto, K., and Kaneda, T. (1987) *J. Am. Oil Chem. Soc. 64*, 876−879.
40. Marnett, L. J., and Wilcox, A. L. (1995) *Biochem. Soc. Symp. 61*, 65−72.
41. Park, J. W., and Floyd, R. A. (1992) *Free Radical Biol. Med. 12*, 245−250.
42. Douki, T., Riviere, J., and Cadet, J. (2002) *Chem. Res. Toxicol. 15*, 445−454.
43. Moriya, M. (1993) *Proc. Natl. Acad. Sci. U.S.A. 90*, 1122−1126.
44. Henderson, P. T., Delaney, J. C., Muller, J. G., Neeley, W. L., Tannenbaum, S. R., Burrows, C. J., and Essigmann, J. M. (2003) *Biochemistry 42*, 9257−9262.
45. Henderson, P. T., Delaney, J. C., Gu, F., Tannenbaum, S. R., and Essigmann, J. M. (2002) *Biochemistry 41*, 914−921.
46. Feig, D. I., Sowers, L. C., and Loeb, L. A. (1994) *Proc. Natl. Acad. Sci. U.S.A. 91*, 6609−6613.
47. Kreutzer, D. A., and Essigmann, J. M. (1998) *Proc. Natl. Acad. Sci. U.S.A. 95*, 3578−3582.
48. Basu, A. K., Wood, M. L., Niedernhofer, L. J., Ramos, L. A., and Essigmann, J. M. (1993) *Biochemistry 32*, 12793−12801.
49. Ham, A. J., Ranasinghe, A., Koc, H., and Swenberg, J. A. (2000) *Chem. Res. Toxicol. 13*, 1243−1250.
50. Jones, W. R., and Dedon, P. C. (1999) *J. Am. Chem. Soc. 121*, 9231−9232.
51. Mlakar, A., and Spiteller, G. (1996) *Chem. Phys. Lipids 79*, 47−53.
52. Saparbaev, M., Kleibl, K., and Laval, J. (1995) *Nucleic Acids Res. 23*, 3750−3755.
53. Saparbaev, M., and Laval, J. (1998) *Proc. Natl. Acad. Sci. U.S.A. 95*, 8508−8513.
54. Miyake, T., and Shibamoto, T. (1996) *Food Chem. Toxicol. 34*, 1009−1011.
55. Feng, Z., Hu, W., Amin, S., and Tang, M. S. (2003) *Biochemistry 42*, 7848−7854.
56. Kawanishi, M., Matsuda, T., Nakayama, A., Takebe, H., Matsui, S., and Yagi, T. (1998) *Mutat. Res. 417*, 65−73.
57. Chung, F. L., Nath, R. G., Ocando, J., Nishikawa, A., and Zhang, L. (2000) *Cancer Res. 60*, 1507−1511.
58. Kawanishi, M., Matsuda, T., Sasaki, G., Yagi, T., Matsui, S., and Takebe, H. (1998) *Carcinogenesis 19*, 69−72.
59. Moraes, E. C., Keyse, S. M., and Tyrrell, R. M. (1990) *Carcinogenesis 11*, 283−293.
60. Akman, S. A., Lingeman, R. G., Doroshow, J. H., and Smith, S. S. (1991) *Biochemistry 30*, 8648−8653.
61. Seidman, M. M., Bredberg, A., Seetharam, S., and Kraemer, K. H. (1987) *Proc. Natl. Acad. Sci. U.S.A. 84*, 4944−4948.
62. Lee, D. H., O'Connor, T. R., and Pfeifer, G. P. (2002) *Nucleic Acids Res. 30*, 3566−3573.
63. Yagi, T., Tatsumi-Miyajima, J., Sato, M., Kraemer, K. H., and Takebe, H. (1991) *Cancer Res. 51*, 3177−3182.
64. Madzak, C., Armier, J., Stary, A., Daya-Grosjean, L., and Sarasin, A. (1993) *Carcinogenesis 14*, 1255−1260.
65. Strauss, B. S. (1997) *Carcinogenesis 18*, 1445−1452.
66. Rodin, S. N., Rodin, A. S., Juhasz, A., and Holmquist, G. P. (2002) *Mutat. Res. 510*, 153−168.
67. Moraes, E. C., Keyse, S. M., Pidoux, M., and Tyrrell, R. M. (1989) *Nucleic Acids Res. 17*, 8301−8312.

BI035555W